Article

Cite This: Biomacromolecules 2018, 19, 2969−2978

pubs.acs.org/Biomac

Transparent, Flexible, and Strong 2,3-Dialdehyde Cellulose Films with High Oxygen Barrier Properties

Sven F. Plappert,[†] Sakeena Quraishi,[†] Nicole Pircher,[†] Kirsi S. Mikkonen,[§] Stefan Veigel,[‡] Karl Michael Klinger,[†] Antje Potthast,[†] Thomas Rosenau,[†] and Falk W. Liebner*[,†]

[†]Division of Chemistry of Renewable Resources and [‡]Institute of Wood Technology and Renewable Resources, University of Natural Resources and Life Sciences Vienna, Konrad-Lorenz-Straße 24, A-3430 Tulln, Austria

[§]Department of Food and Environmental Sciences, University of Helsinki, P.O. Box 27, Helsinki, Finland

ABSTRACT: 2,3-Dialdehyde cellulose (DAC) of a high degree of oxidation (92% relative to AGU units) prepared by oxidation of microcrystalline cellulose with sodium periodate (48 °C, 19 h) is soluble in hot water. Solution casting, slow air drying, hot pressing, and reinforcement by cellulose nanocrystals afforded films (∼100 μm thickness) that feature intriguing properties: they have very smooth surfaces (SEM), are highly flexible, and have good light transmittance for both the visible and near-infrared range (89−91%), high tensile strength (81−122 MPa), and modulus of elasticity (3.4−4.0 GPa) depending on hydration state and respective water content. The extraordinarily low oxygen permeation of <0.005 cm^3 μm m^{-2} day^{-1} kPa^{-1} (50% RH) and <0.03 cm^3 μm m^{-2} day^{-1} kPa^{-1} (80% RH) can be regarded as a particularly interesting feature of DAC films. The unusually high initial contact angle of about 67° revealed a rather low hydrophilicity compared to other oxidatively modified or unmodified cellulosic materials which is most likely the result of inter- and intramolecular hemiacetal and hemialdal formation during drying and pressing.

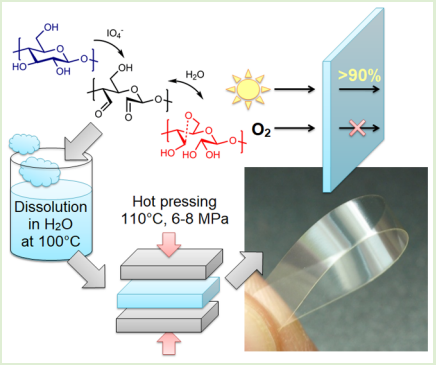

INTRODUCTION

The increasing use of renewable resources for the manufacture of everyday materials, commodities, or cutting-edge products—either indirectly in the form of synthetic building blocks obtained by preceding transformation of biomass into chemicals or directly employing specific properties inherent to natural polymers—is an important goal of current resource utilization strategies.[1,2] Cellulose with an estimated annual renewal rate of 7.5 × 10^{10} tons[3] attracts particular attention in this respect and has always found broad utilization in our daily life either in unmodified (fiber, paper, tissue, cosmetic, and medical applications) or in chemically modified form of cellulose derivatives (thickeners, adhesives, membrane materials, films, fibers, etc.).

Periodate oxidation of cellulose, which involves the selective conversion of the two secondary hydroxyl groups in C2 and C3 positions of the anhydroglucose units (AGU) into aldehyde moieties and concomitant cleavage of the respective carbon−carbon bond, is a well-known method of cellulose modification and has been applied for structural analyses of poly- and oligosaccharides and their substitution patterns.[4] However, even though the properties of cellulose can be greatly altered already at low degrees of modification,[5] periodate oxidation of cellulose has hitherto not yet been implemented on a large commercial scale. This is mainly due to the high price of sodium periodate and its toxicity, both calling for environmentally safe and quantitative recycling of the oxidant, and the limited solubility (and workability) of 2,3-dialdehyde cellulose (DAC) limiting its homogeneous processing. However, it might be reasonably assumed that DAC will soon conquer the bio-based materials market as recent studies have shown that sodium periodate can be efficiently regenerated using ozone in strongly alkaline medium.[6] Furthermore, 2,3-dialdehyde cellulose can afford homogeneous solutions in hot water[7,8] provided a sufficiently high degree of oxidation. Both results have boosted research related to the utilization of DAC in new products. In particular, the ability of DAC to form primary (R^1−CH═NH) or secondary aldimines (R^1−CH═N−R^2) and Schiff bases (R^1−CR^3═N−R^2) affords possibilities galore for further chemical modification including cross-linking. This renders DAC an interesting source material for a broad range of applications, in particular those that require covalent immobilization of high-molecular-weight nitrogenous compounds. The latter comprise for example polypeptides and proteins including enzymes,[9−12] antibodies,[11,13] collagen,[14−16] gelatin,[17,18] oligonucleic acid aptamers,[19] chitosan,[20,21] or polyallylamines.[22] Enzymes immobilized on DAC can be employed for example in enzyme-enhanced wastewater treatment[9] or wound healing.[10] DAC has been also tested as substrate for highly sensitive electrochemical immune[13] and aptamer sensors.[19] It has been also used as host matrix for covalently immobilized upconverting nanoparticles serving as

Received: March 29, 2018
Revised: May 8, 2018
Published: May 14, 2018

DOI: 10.1021/acs.biomac.8b00536
Biomacromolecules 2018, 19, 2969−2978

sensors in resonance energy transfer nucleic acid hybridization assays.[23] Lower-molecular-weight compounds, such as hydroxylamine,[24,25] butylamines,[26−28] or 1,12-diaminododecane,[26] have been coupled with DAC as well to afford superhydrophobic[26] or amphiphilic materials[27] depending on their aliphatic chain lengths.

Its bioresorbability and biodegradability render DAC attractive for medical applications, too, where it could be exploited as matrix material for controlled release of drugs,[29] cell scaffolding material for tissue engineering,[16,30,31] wound dressing,[16,32] or surgical material.[32]

As outlined above, shaping of 2,3-dialdehyde cellulose from solution state is not trivial due to its insolubility in organic solvents or cold water, even if cellulose is completely oxidized. This specific solubility problem has been ascribed to the multitude of intra- and intermolecular hemiacetal and -aldal moieties formed from the newly introduced aldehyde and remaining hydroxyl groups[7,33,34] as well as the resulting cross-linking effects.

Dissolution of 2,3-dialdehyde cellulose in hot water (>80 °C) as reported by Kim et al.[7] for DAC of high degree of oxidation (DO > 90%) is hitherto the only way to process DAC from solution state, which is, however, also limited to certain conditions and techniques.

This study investigated solution casting of aqueous 2,3-dialdehyde cellulose of high degree of oxidation (92% related to the number of anhydroglucose units, AGU) and the properties of the resulting products. Particular emphasis was put on recyclability and environmental compatibility of the processes involved. To this end microcrystalline cellulose and cellulose nanocrystals were used as bulk and reinforcing source materials, respectively; water was the only medium for synthesis and processing, and sodium periodate as an oxidant can be almost quantitatively recycled with the green oxidant ozone (see above). The prepared films were subjected to comprehensive material characterization and testing, including Fourier-transform infrared spectroscopy (FTIR), elemental analysis, scanning electron microscopy (SEM), thermal analysis (DMA and DSC), light transmittance and contact angle measurements, oxygen barrier analysis, and tensile testing.

MATERIALS AND METHODS

Materials. All chemicals were purchased from Sigma-Aldrich (Vienna, Austria) and used without further purification. Cellulose nanocrystals (CNC), obtained by treating wood pulp with 64% sulfuric acid to hydrolyze the amorphous regions of cellulose, were purchased from the University of Maine, Process Development Center, and manufactured at the US Forest Service's Cellulose Nanomaterials Pilot Plant in the Forest Products Laboratory (Madison, WI). The dimensions of such nanocrystals are approximately 5 × 150−200 nm, corresponding to aspect ratios of 30 to 40.[35] Microcrystalline cellulose (MCC, Avicel PH-101) with a particle size of 50 μm was used as the cellulose source.

Periodate Oxidation of Cellulose. A suspension of 24 g of Avicel PH-101 in 1000 mL of deionized water was prepared in a 2000 mL Schott bottle. The bottle was then carefully wrapped with aluminum foil to prevent light-induced decomposition of periodate. 38.025 g of sodium metaperiodate ($NaIO_4$; 1.2 molar excess related to anhydroglucose units; AGU) was dissolved in 484 mL of deionized water and added to the suspension. The bottle was placed in a water bath at 48 °C and stirred at 1000 rpm. After 19 h the reaction was stopped by decantation and subsequent thorough washing of the oxidized cellulose with deionized water. The solid content of the wet filter residue was determined using a Sartorius MA35 (Göttingen, Germany) moisture balance. Never-dried DAC was then dispersed in deionized water to give a solid content of 10% w/v and stored under a nitrogen atmosphere at 4 °C until further processing.

Analysis of Degree of Oxidation. The degree of cellulose oxidation (DO) was approximated indirectly by photometric quantification of the consumed amount of periodate. This has been accomplished by measuring the UV absorption (λ_{exc} 290 nm,[36] Lambda 35 UV/vis spectrometer, PerkinElmer, Waltham, MA) of a 40-fold diluted aliquot taken from the reaction mixture 19 h after the oxidation had been started. The DO was calculated as the percentage of oxidized AGUs compared to the total number of AGUs.

Film Formation. A 10% w/v aqueous suspension of never-dried 2,3-dialdehyde cellulose was heated to 100 °C for 45−60 min under continued stirring (1400 rpm). Centrifugation of the hot solution at 6000 rpm for 10 min removed small quantities of insolubles. The resulting clear DAC solution was transferred into polystyrene molds (box-shaped with a base of about 10 × 10 cm) and slowly dried in a ventilated oven at 35 °C for 2−3 days. Selected samples were carefully placed between two paper sheets and ironed (ca. 140 °C) from both sides using a household pressing iron to remove wrinkles and residual water.

Reinforcement of DAC Films with CNC. A 7.2% w/v aqueous dispersion of CNC was added to the 10% w/v aqueous solutions of DAC to yield a 5 wt % CNC containing DAC composite after drying (referred to as DAC/CNC films). Film formation was achieved according to the above procedure. The CNC reinforced samples were characterized by SEM, tensile testing, oxygen barrier analysis, and light transmittance measurement.

Pressing of DAC Films. Selected DAC film samples were pressed using a Langzauner press LZT-OK 175 (Lambrechten, Austria). After preheating the equipment to 110 °C (boiler temperature 150 °C), the films were pressed between two plates at 110 °C for 10 min. The applied pressure was adjusted to deliver a pressure of 6−8 MPa to the films. The press was cooled down to room temperature by a water cooling system before the samples were withdrawn.

Characterization of DAC Films. *Elemental Analysis.* The carbon, hydrogen, sulfur, and nitrogen contents of DAC films (equilibrated at 50% RH) were measured in duplicate using an EA 1108 CHNS-O instrument (Thermo Scientific/Carlo Erba, USA). Oxygen contents were analyzed with an Eurovector EA 3000 (Pavia, Italy) combined with a high-temperature pyrolysis unit (Hekatech, Wegberg, Germany). Potential remnants of iodine species in the formed films were quantified by inductively coupled plasma mass spectrometry (ICP-MS). Prior to ICP-MS analysis, the samples were digested in a mixture of 5 mL of 69% HNO_3 and 1 mL of 30% H_2O_2 at 155 °C under constant stirring for 4 h. The obtained solution was adjusted to about 30 mL by adding distilled water and further diluted in the ratio 1:5. The sample was then analyzed in duplicate by ICP-MS (Elan DRCe 9000, PerkinElmer, Waltham, MA) using indium nitrate as an internal standard.

Moisture Content. DAC films were either dehydrated (DH-DAC films) by drying over P_4O_{10} or equilibrated at 65% relative humidity (RH, referred to as DAC films) to investigate the effect of residual water, possibly effecting hydration of aldehyde groups and formation of hemialdal moieties. Therefore, fresh DAC films were stored for 16 days at about 21 °C in desiccators containing either an oversaturated solution of NH_4NO_3 (65% RH) or P_4O_{10} in powder form (0% RH). After equilibration and determination of the water content, all samples were subjected to mechanical testing and FTIR analysis. Relative humidity and temperature were monitored by DL-120TH data loggers (Voltcraft, Wollerau, Switzerland) which were placed inside the desiccators.

Water content analysis was accomplished by immersing defined quantities of chopped DAC films (ca. 125 mg) in 1 mL of absolute ethanol and incubation of the mixture under shaking for 25 h. Quantification of the amount of water absorbed by absolute ethanol was accomplished by Karl Fischer titration using a V20 Volumetric KF Titrator (Mettler Toledo, Columbus, OH). The same method of moisture determination was applied to the films analyzed by elemental analysis and ICP-MS.

DOI: 10.1021/acs.biomac.8b00536
Biomacromolecules 2018, 19, 2969−2978

Chemical Structure. Fourier transformation infrared spectroscopy (FTIR) on samples equilibrated at 0 and 65% RH (see above) was performed on a PerkinElmer Frontier FTIR spectrometer (Waltham, MA) using the attenuated total reflection (ATR) mode (4000 to 650 cm^{-1}, 16 scans). For the sake of comparison, samples of the parent microcrystalline cellulose (MCC; Avicel PH-101) prior to and after periodate oxidation were included. The oxidized MCC was freeze-dried prior to FTIR analysis. All FTIR spectra were baseline corrected and normalized to the C−H stretching band identified as the maximum between 3000 and 2500 cm^{-1}.

Size Exclusion Chromatography (SEC). SEC was used to evaluate the molecular weight of 2,3-dialdehyde cellulose and the loss of molecular weight caused by periodate oxidation and dissolution in hot water as previously described.[37]

SEC measurement of nonoxidized MCC was performed with DMAc/LiCl (9% w/v) as the cellulose solvent and DMAc/LiCl (0.9% w/v) as the mobile phase. The SEC system consisted of the following components: online degasser, Dionex DG-2410; pump, Kontron 420 with pulse damper; autosampler HP 1100 (Agilent Technologies, Santa Clara, CA); column oven, Gynkotek STH 585; MALLS detector, (Wyatt Technologies, Santa Barbara, CA, Dawn DSP) with argon ion laser (λ_0 = 488 nm); RI detector, Shodex RI-71. The following parameters were used for SEC measurements: flow: 1.00 mL min^{-1}; columns: four PL gel mixed A LS, 20 μm, 7.5 × 300 mm; injection volume: 100 μL; run time: 45 min.

For DAC analysis, sample preparation was accomplished by dissolving 1 wt % of never-dried periodate-oxidized cellulose in boiling water. Prior to analysis, 0.1 M NaCl was added, and the samples were filtered using a 0.45 μm PTFE syringe filter. The SEC system consisted of a pump equipped with DG-1210 online degasser (Dionex, Sunnyvale, USA) and G1367C autosampler (Agilent Technologies, Santa Clara, CA). The sample was chromatographed on three SEC columns (Agilent PL Aquagel-OH Mixed-H, pore size, 8 μm) and monitored by MALLS (DAWN HELEOS with 120 mW solid-state laser operating at 658 nm, Wyatt Technologies, Santa Barbara, CA), dynamic light scattering (DynaPro NanoStar, Wyatt Technologies, Santa Barbara, CA), and RI (T-rEX, Wyatt Technologies, Santa Barbara, CA) detectors. The following system parameters were used: 0.8 mL min^{-1} flow rate; 100 μL injection volume; 40 min run time. Data collection and molecular weight calculations were performed by ASTRA software Version 6.0.1. All measurements were carried out at room temperature.

Surface Morphology. Scanning electron microscopy (SEM) of film surfaces and breaking edges was performed on gold-sputtered samples (EM SCD005 sputter coater, Leica, Wetzlar, Germany; layer thickness 6 nm) using a Tecnai Inspect S50 (FEI, Hillsboro, OR) instrument under high vacuum at an acceleration voltage of 10.00 kV.

Mechanical Response toward Tensile Stress. The tensile strength of the film samples was measured on a Zwick-Roell Materials Testing Machine Z020 (Ulm, Germany) using a 500 N load cell and an extension rate of 1 mm min^{-1}. An initial load of 1 N mm^{-2} was applied. The modulus of elasticity (E_{mod}) was determined by linear regression between 10% and 40% of the maximum force. The toughness (U_T) was defined as the integral over the respective stress−strain curves. The clamping length was 20 mm, and the film samples used for tensile testing were about 5 mm wide. The impact of the DAC water content on mechanical properties was investigated using the same sets of samples equilibrated for 16 days at 0 and 65% RH, as used for FTIR studies. DAC films reinforced with CNC were prepared in a similar way (65% RH, 20 °C) but only equilibrated for 5 days prior to the measurement.

Dynamical Mechanical Analysis (DMA). DMA was carried out under a N_2 atmosphere using a Netzsch DMA 242 C instrument (Selb, Germany). The heating rate was 3 °C min^{-1}, and the temperature range was −40 to 150 °C. Dynamic force was applied at a frequency of 1 Hz. Cooling to −40 °C prior to the measurement was performed at a rate of 10 °C min^{-1} with an equilibration time of 3 min. The clamping length was 10 mm, and the maximal amplitude was set to 10 μm, allowing a maximum elongation of 1%. The maximum dynamic force was set to 4 N, which was sufficient to achieve 1% elongation at each temperature. DMA was carried out on an unpressed DAC film, 203 μm thick and 3.463 mm wide, which had been stored at 20 °C and 65% RH for 3 days prior to measurement.

The obtained storage modulus (E') curve was smoothed by Savitzky Golay operation (part of Origin Pro software package, Northampton, MA) using a 100 data point window. The curve of the static length change (dL) was smoothed using a 50 data point window FFT filter.

Differential Scanning Calorimetry (DSC). DSC was performed on a DSC 821e instrument (Mettler-Toledo, Columbus, OH) equipped with a liquid nitrogen cooling unit. Measurements were conducted on unpressed DH-DAC and DAC film fragments placed into 160 μL aluminum crucibles with 50 μm holes in the lids. Temperature program (two heating and cooling cycles): heating from 0 to 110 °C at 1 °C min^{-1}; hold for 5 min; cooling to 0 °C at 1 °C min^{-1}; 5 min hold; heating to 137 °C at 1 °C min^{-1}, hold for 5 min, cooling to 0 °C at 1 °C min^{-1}.

Light Transmittance. Light transmittance of both unpressed and pressed DAC films as well as of a pressed DAC/CNC film (DAC film reinforced with 5 wt % of CNC) was studied in the wavelength range between 1000 and 200 nm using a scanning speed of 8 nm s^{-1} (Lambda 35 UV/vis spectrometer, PerkinElmer, Waltham, MA).

Oxygen Barrier Analysis. The oxygen gas transmission rate (OTR) of both unpressed and pressed DAC films as well as of pressed DAC/CNC films was measured using an oxygen permeability (OP) analyzer equipped with a coulometric sensor (M8001; Systech Illinois, Oxfordshire, UK). The films were exposed to 100% oxygen atmosphere on the one side and to oxygen-free nitrogen on the other side. The OP was calculated by multiplying the OTR by the thickness of the film and dividing it by the oxygen gas partial pressure difference between the two sides of the film. The measurements were carried out at 23 °C, atmospheric pressure, and relative humidities of 50% and 80%. The specimen area was 5 cm^2, and the thickness of the film was measured before analysis at five points using a L&W Micrometer (Lorentzen & Wettre, Kista, Sweden) at 1 μm precision. The OP was determined in duplicate. The OTR and OP were determined using individual zeroing, which is assumed to afford more accurate data than a normal baseline correction and is recommended for high barrier films.

Contact Angle Measurements. The contact angle (θ_C) of unpressed DAC films was measured using a setup composed of a CCD camera device (Sony 93D, Model XC-77CE, 2/3 Zoll CCD, 11 × 11 μm pixel size) and an adjustable background lighting under controlled temperature (23 °C) and relative humidity (50% RH). The measurements were performed with distilled water. A 8 μL drop was applied by a manual precision dosage system. The angle between water drop and surface was determined with DSA1 drop shape analysis software (KRÜSS Optronic GmbH, Hamburg, Germany). The θ_C measurement was started 15 s after the droplet had been deposited onto the surface of the respective films and was repeated every 20 s for a time period of 20 min.

RESULTS AND DISCUSSION

Oxidation of Cellulose. The rate of cellulose oxidation to 2,3-dialdehyde cellulose (DAC) by sodium periodate in aqueous medium is mainly controlled by the factors temperature and periodate concentration.[38] Since periodate decomposes noticeably beyond 55 °C under concomitant liberation of iodine which, in turn, can engage in side reactions with cellulose and the DAC formed,[39] the oxidation temperature in this study was set to 48 °C as a compromise between still satisfyingly high reaction rate[38] and sufficiently low iodine generation.

The degree of oxidation (DO) for the microcrystalline cellulose used in this study was 92% after a reaction time of 19 h which turned out to be optimum with regard to the combination of good solubility of the resulting 2,3-dialdehyde cellulose in hot water (90 °C) and low degradation by overoxidation. It was calculated from periodate consumption as

DOI: 10.1021/acs.biomac.8b00536
Biomacromolecules 2018, 19, 2969−2978

proposed by Kim and Kuga,[24] who demonstrated its similarity to alkali consumption in Cannizzaro reactions.[24] Oximation or hydrazonation of the newly introduced aldehyde moieties and subsequent titration or quantification of the nitrogen content by elemental analysis would have been other, but more laborious, alternatives.

On the basis of previous studies investigating the kinetics of periodate oxidation of various polysaccharides such as amylose[43,45,46] and C6-oxycellulose,[47] it is suspected that immediately after the oxidation of an AGU the newly introduced aldehyde groups at the C2 and C3 positions participate in intra- and/or intermolecular hemiacetal ring formation (presumably five-, six-, and/or seven-membered). The latter are in an equilibrium state with hemialdal structures, and the free as well as solvated (hydrated) aldehyde forms. This is also supported by the findings of Mester,[44] who investigated several polysaccharides, which were oxidized with periodic acid, including cellulose, starch, inulin, xylan, and dextrin. Furthermore, intermolecular hemiacetals bridges can potentially be formed with OH groups at the C2 or C3 positions of neighboring, not oxidized AGUs and act as temporarily active protecting groups toward periodate oxidation through an autoinhibition effect.[46,48]

In addition to the above-described intramolecular interactions comprising the potential structural moieties shown in Figure 1, the formation of intermolecular hemiacetal cross-links

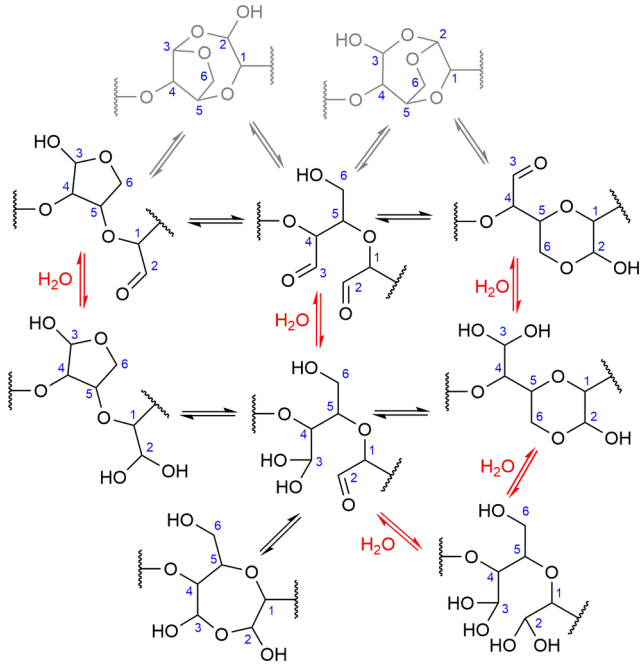

Figure 1. Chemical structures of a single periodate oxidized anhydroglucose unit potentially occurring in the transition between solution, gel, and solid state without considering additional intermolecular links (based on refs 8, 34, and 40−44). Gray structures propose bicyclic intramolecular hemiacetal structures; red equilibria arrows emphasize the role of water in DAC processing.

is likely for cellulose samples of high carbonyl content exceeding 60−80 mmol kg^{-1} as proposed by Potthast et al.[33] and Morooka et al.[34] The existence of both intra- and intermolecular hemiacetal moieties in aqueous solutions of 2,3-dialdehyde cellulose has been recently confirmed by NMR studies.[8]

As a result of successive cleavage of pyranose rings and hydrogen bonds, periodate oxidation of cellulose results in both decreasing degree of crystallinity and increasing macromolecular flexibility until the material becomes completely amorphous at DO values exceeding 87%.[24]

Table 1. SEC Results for Avicel and DAC

	Avicel	DAC	
	peak 1	peak 2	peak 1
mass [%]	100	98.27	1.73
M_w [g mol^{-1}]	38630 (±0.7%)	5929 (±0.390%)	6648000 (±0.612%)
M_z [g mol^{-1}]	68170 (±0.4%)	6365 (±0.879%)	7710000 (±1.229%)
M_w/M_n	2.040 (±0.8%)	1.062 (±0.409%)	1.322 (±0.191%)
M_z/M_n	3.601 (±1.2%)	1.134 (±0.702%)	1.678 (±0.317%)

Size exclusion chromatography of the obtained 2,3-dialdehyde cellulose (DAC) showed a molar mass distribution containing two fractions. The main part (98.3 wt %) of the material exhibited a weight-average molecular weight (M_w) of 5.9 kg mol^{-1} at a low polydispersity of about 1.06 and had therefore undergone heavy degradation by about 85% compared to the starting material (38.6 kg mol^{-1}). A second, small fraction (1.7 wt %) contained probably aggregates with M_w as high as ∼6650 kg mol^{-1}.

Film Formation. The obtained aqueous DAC solutions were inviscid at 10% w/v concentration but formed a gel upon slow drying (35 °C, 24 h) of the solution-cast samples in a convection oven. This gel state could be preserved for several weeks if the drying process was stopped and the gel was stored at sufficiently high humidity (98% RH). Upon further drying, the gel structure compacted to a dense and solid film. The relatively low drying temperature of 35 °C was chosen because in advanced stage of film formation the material becomes increasingly prone to contraction, curling, and deformation, which is also reflected by the ΔL values recorded by DMA when water is removed during the heating step. It is therefore mandatory to maintain a homogeneous water distribution during drying. Ironing of DAC sheets as accomplished for preliminary testing caused curling, too. However, alternating ironing from both sides turned out to be effective at counteracting deformation. The necessity to maintain a low increment of decreasing water content during drying also limited the achievable thickness of the prepared films and sheets. The samples prepared in this study were between 50 and 220 μm thick, and the majority of samples subject to comprehensive material testing had a thickness of about 100 μm if not mentioned otherwise. It is worth noticing that DAC films can be redissolved in hot water provided they are first ground into small particles. This way, new films can be formed, allowing for quantitative recycling of the material.

Considering that the formed aldehyde moieties almost quantitatively engage in intra- and intermolecular hemiacetal and hemialdal formation which was confirmed by respective analysis (see below), we concluded that cellulose nanocrystals (CNC)—a material which is increasingly used for reinforcement of polymers[49−51]—should be particularly well covalently incorporated to afford an *all*-cellulose composite material, DAC/CNC. This has been tested by adding CNC to the aqueous DAC solution to yield films reinforced with 5 wt % CNC.

Chemical Structure of DAC Films. FTIR analysis of freeze-dried DAC revealed the chemical structure of DAC in

DOI: 10.1021/acs.biomac.8b00536
Biomacromolecules 2018, 19, 2969−2978

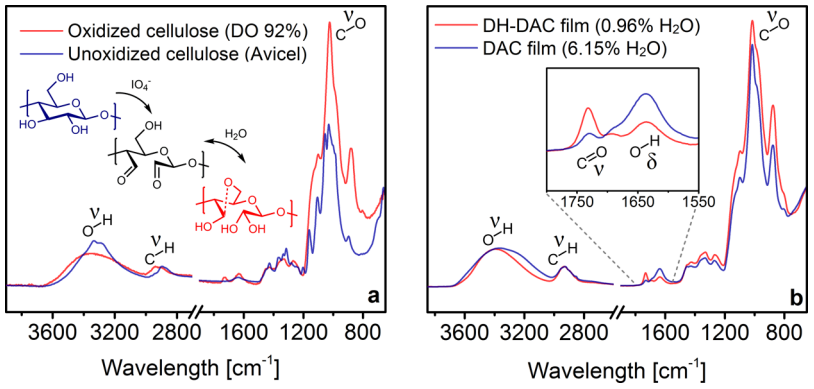

Figure 2. (a) FTIR spectra of MCC (Avicel PH-101) and the washed and freeze-dried DAC obtained thereof by periodate oxidation. (b) Pressed DH-DAC and DAC films (equilibrated at 0% and 65% RH for 16 days).

Table 2. Elemental Composition (wt %) of DAC Films (5.77 wt % Water Content) Obtained from Periodate-Oxidized Microcrystalline Cellulose (92% DO)

	C	H	N	S	O	∑C,H,N,S,O
analyzed	38.8 ± 0.05	5.7 ± 0.18	<0.05	<0.02	54.4 ± 0.13	99.0
calculated	40.2	5.7	0.0	0.0	54.1	100.0

solid state considerably to differ from that of the parent microcrystalline cellulose and to be dominated by C−O−C bonds as reflected by ν_{C-O} vibrations at 800−1030 cm^{-1} (Figure 2). Strong periodate oxidation led to only a very moderate decrease of O−H stretching (ν_{OH}, 3000−3600 cm^{-1}) signals accompanied by significant peak broadening; even a very slight increase was observed for the adsorbed water signal at 1641 cm^{-1}, which shifted to 1635 cm^{-1} for the oxidized cellulose, possibly indicating aldehyde hydration. Furthermore, a strong increase of the C−O signals occurred in the C−O−C region between 986 and 1030 cm^{-1}, especially for the C−O−C valence vibration, represented by the peaks at 897 cm^{-1} (MCC) and 884 cm^{-1} (oxidized cellulose). Signals caused by free aldehydes are hardly detected and limited to a weak carbonyl stretch vibration band ($\nu_{C=O}$, 1732 cm^{-1}), since most aldehyde groups are engaged in their masked forms of hemiacetals, hydrates, and hemialdals.[41]

The DAC dissolution and film formation processes resulted in an increase of the C−O−C valence vibration (876−884 cm^{-1}), suggesting the formation of even more hemiacetal and hemialdal moieties compared to the washed and freeze-dried, crude oxidized MCC. Additionally, a slight decrease of free aldehyde ($\nu_{C=O}$) moieties is effected by the film-forming process. Also, the structural differences attributed to the different moisture contents of the pressed DH-DAC and DAC films (0.96 wt % for films equilibrated over P_4O_{10}; 6.15 wt % for films stored at 65% RH) are visible in the FTIR spectra as evident from Figure 2. By removing water through drying over P_4O_{10}, fewer aldehyde groups can persist in a hydrated state, which changes the equilibrium in the DAC films toward free aldehyde groups and likely bicyclical hemiacetal structures. Drying of the DAC films over P_4O_{10} for 16 days resulted in a decrease of the water content from about 6 to 1 wt %, causing doubling of the weak C═O carbonyl stretch signal as well as an increase of the C−O−C signal.

With regard to the chemical structure of the DAC films formed by solution casting, the following conclusions can be drawn: The material is completely amorphous[24] (this is also indicated by the broadening of ν_{OH} signal upon oxidation) because about 92% of the AGUs are oxidized which imparts the largely open-chain polyether backbone (only about every tenth AGU remains unaltered by periodate oxidation) with potentially high flexibility. However, the two aldehyde moieties and one methylol group attached to each of the oxyethylenoxymethyl repeating units constituting the open-chain DAC blocks restrict this flexibility by (random) formation of cyclic presumably five-, six-, and seven-membered, intra- and intermolecular hemiacetal and hemialdal structures, which exist in equilibrium with some hydrated and free aldehyde groups.[33,34] The amount of the latter cannot be high: only very weak $\nu_{C=O}$ signals (1732 cm^{-1}) from carbonyl stretching vibrations were found in the FTIR spectra besides the dominating, strong C−O−C signals (hemialdals and -acetals). These results are in good agreement with a previous study of the stability and aging of solubilized dialdehyde cellulose of high degree of oxidation which confirmed the prevalent (intramolecular) hemiacetal structure of DAC in solution and the maintained functionality of the masked aldehyde moiety.[8]

Elemental Composition of DAC Films. The results of elemental analysis of a DAC film equilibrated at 50% RH (Table 2) were in good agreement with its theoretical elemental composition which was calculated assuming 92% degree of oxidation (based on periodate consumption) and considering the actual water content (5.77 wt %). The latter was determined immediately before elemental analysis by consecutive extraction of film fragments with absolute ethanol and quantification of its water content by Karl Fischer titration. The results confirm that the applied extraction method, i.e., immersion of a well-known amount of DAC film in a defined volume of absolute ethanol, is capable to desorb quantitatively both free moisture and even water bound to DAC in form of aldehyde hydrates as proposed for example by Mester.[44] This supports the theory of Painter and Larsen[45] which proposes that the aldehyde groups in DAC exist in an equilibrium state which includes free and hydrated forms as well as various hemiacetal and hemialdal structures (cf. Figure 1). Considering the comparatively low water content of the studied DAC film (5.77 wt %) which corresponds to about 0.5 mol equivalents of

DOI: 10.1021/acs.biomac.8b00536
Biomacromolecules 2018, 19, 2969−2978

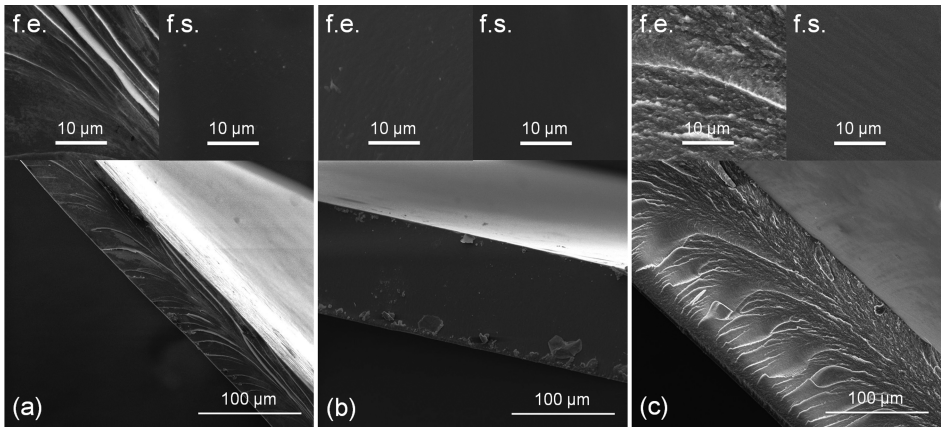

Figure 3. Scanning electron micrographs of film surfaces (f.s.) and breaking edges (f.e.) of unpressed (a), pressed (b), and pressed DAC films containing 5 wt % CNC (c); the respective bigger pictures depict an angled view of a breaking edge of the films while the smaller pictures labeled f.e. and f.s. show edges and surfaces of the films at higher magnification from an orthogonal viewpoint.

Table 3. Mechanical Properties of DAC and *All*-Cellulose DAC/CNC Composite Films of Different Water Contents under Tensile Stress (n = 4): Modulus of Elasticity (E_{mod}), Ultimate Strength (UTS), Elongation at Break (dL at F_{max}), and Toughness (U_T)

H_2O [wt %]	CNC [wt %]	E_{mod} [GPa]	UTS (σ_M) [MPa]	dL at F_{max} [%]	U_T [J m^{-3}·10^4]
1	0	3.41 ± 0.16	122.46 ± 4.96	7.23 ± 1.06	603.20 ± 137.89
6	0	4.03 ± 0.09	80.92 ± 8.09	2.24 ± 0.34	103.33 ± 25.31
7	5	4.70 ± 0.23	120.91 ± 3.00	2.82 ± 0.21	172.68 ± 21.04

total aldehyde moieties present in the DAC films, hydration of aldehyde groups is evidently limited. In context with the weak FTIR signal at $\nu_{C=O}$ 1732 cm^{-1} indicating the presence of only a few free aldehyde groups, it is reasonable to conclude that the majority of aldehyde groups becomes "masked" by hemiacetal and hemialdal formation during film formation. This process is assumed to be reversible as the DAC films formed can be redissolved allowing for quantitative recycling of DAC-based materials.

Elemental analysis did not indicate any nitrogen- or sulfur-containing impurities. The iodine content of the films determined by ICP-MS was as low as 12−20 μg g^{-1}, confirming that the reagent was sufficiently well removed from the crude DAC by the applied postoxidation washing procedure.

Morphology of Unpressed, Pressed, and Reinforced DAC Films. Scanning electron microscopy (SEM) showed very smooth surfaces for all the studied samples, no matter whether the DAC films were pressed, blending with 5 wt % of cellulose nanocrystals prior pressing, or directly analyzed after drying of the solution-cast films (Figure 3, film surfaces; f.s.). The SEM study confirmed the absence of any pores at the micrometer and submicrometer scale. The highly uniform film matrix is obviously the result of the full disintegration of crystalline domains in the microcrystalline starting material caused by the heavy periodate oxidation,[52] the homogeneous dissolution of the obtained 2,3-dialdehyde cellulose in hot water, and the extensive DAC networks formed by intra- and intermolecular cross-linking via hemiacetal and hemialdal moieties. Exceptionally smooth fracture planes were obtained for the highly compact, pressed DAC films (Figure 3b) while DAC films with 5 wt % CNC being added (prior to solution casting, drying, and hot pressing) and unpressed DAC films yielded somewhat irregular fracture edges (f.e.; Figure 3a,c).

Mechanical and Thermal Properties. Pressed DH-DAC and DAC film samples as well as the pressed DAC/CNC film (reinforced with 5 wt % CNC, 5 × 120−150 nm) were subject to tensile testing to study the impact of water content. The degree of hydration of aldehyde groups has a great influence on the extent of hemiacetal and hemialdal network formation and reinforcement on mechanical properties (cf. Tables 2 and 3).

Pressed DH-DAC films (equilibrated over P_4O_{10} for 16 days; ∼1 wt % water content) showed elastic behavior below 1% elongation and then very slowly and gradually started to deform plastically until the samples broke at around 7% elongation and 122.5 MPa stress. In comparison, regular pressed DAC films (exposed to 65% RH; ∼6 wt % water content), which had a higher modulus of elasticity but substantially lower ability for plastic deformation, featured lower ultimate strength (UTS) and elongation at break (dL; cf. Table 2). While the modulus of elasticity was lower for DH-DAC films they exhibited increased plastic deformation (more than 3-fold elongation before break), which renders the DH-DAC films more ductile. As a consequence, the material becomes more than 5 times tougher compared to regular DAC films.

Considering the rather low molecular weight (∼6000 g mol^{-1} after dissolution in water[8,37]) and amorphous nature of DAC, it may well be assumed that the rather strong and stiff mechanical properties obtained for all DAC films, in particular the extraordinarily high Young's modulus (E_{mod} 3.4−4.0 GPa), are a result of the interlinking hemiacetal and hemialdal structure. The formation of the latter is supported by the presence of water while, presumably reversible, dehydration of the films runs through a softening stage (see below). However, both DH-DAC and DAC films exceeded all expectations with regard to mechanical properties by far. Compared to established commercial polymers like poly(ethylene terephthalate)[53] (PET, UTS 50 MPa, E_{mod} 1.7 GPa), polycarbonate[54] (PC, Lexan 141, UTS 70 MPa, E_{mod} 2.4 GPa), and poly(L-lactide)[55] (PLLA, UTS 28−50 MPa, E_{mod} 1.2−3 GPa), the DAC-based films feature higher stiffness and tensile strength.

DOI: 10.1021/acs.biomac.8b00536
Biomacromolecules 2018, 19, 2969−2978

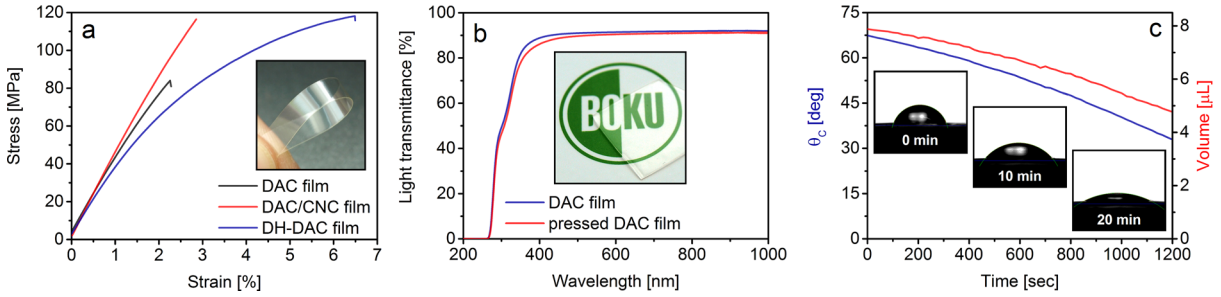

Figure 4. (a) Response of DH-DAC, DAC, and DAC/CNC films toward tensile stress (inset: picture demonstrating the pliability of a DAC film). (b) Light transmittance of a 128 μm thick DAC film prior to and after pressing (inset: picture of DAC film; logo: © BOKU Wien, slightly modified by photographic angle and birefringence of DAC film). (c) Time-resolved change of contact angle and volume of a water droplet deposited on an unpressed DAC film.

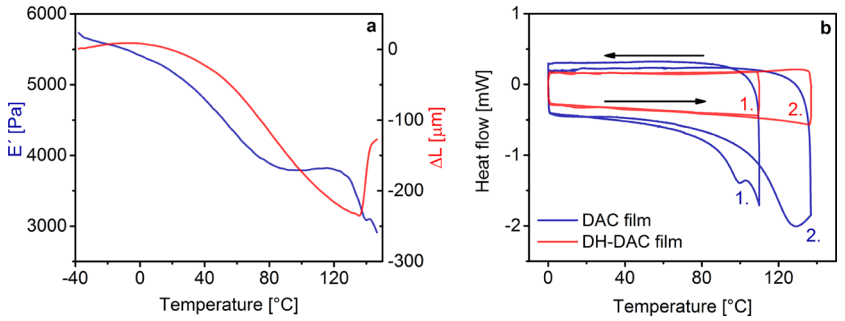

Figure 5. Storage modulus (E'), dimensional change (ΔL), and heat flow of DAC films as obtained by dynamic mechanical analysis (a) and differential scanning calorimetry (b).

Addition of 5 wt % CNC to the DAC solution prior to solution casting, drying and hot pressing had the desired reinforcement effect and further increased both Young's modulus (4.70 vs 4.03 GPa) and ultimate tensile strength (120.9 vs 80.9 MPa) compared to their nonreinforced counterparts while plastic deformation was similarly low considering the somewhat higher water content of the composite film (ca. 7 vs 6 wt % H_2O). On the basis of these findings, it is safe to conclude that cellulose nanoparticles, such as the used CNC, are highly compatible with DAC and well integrated into the 2,3-dialdehyde cellulose networks formed. Their surface hydroxyl groups can participate in the intermolecular hemiacetal formation with DAC affording mechanically very strong *all*-cellulose composite films. Owing to the well-known rigidity of CNC particles, very stiff materials nearly incapable of plastic deformation are obtained this way.

Storage modulus (E') curves obtained by dynamic mechanical analysis (DMA) revealed the stiffness of DAC films to drop in two steps upon heating, being evident from the inflection points at 55.5 and 137.4 °C (Figure 5a). The first broad event occurring below 100 °C is most likely caused by dehydration and loss of water during the heating phase. This is accompanied by a softening of the film by about 30%, which is in accordance with the lower modulus of elasticity of dried films determined by tensile tests (cf. Table 3) compared to films of higher residual water content.

At temperatures above 120 °C the material begins to soften even more in a second transition centered at around 137 °C. The static length change (dL) decreases during the heating up to the second transition point. The total length change is 2.4% between the maximum of dL at −4.33 °C and its minimum at 135.6 °C. This is unusual at a first glance since most materials expand with increasing temperature. However, the contraction seems plausible, since the loss of water during heating is assumed to shift the complex equilibrium between free aldehyde groups, hydrated species, and inter- and intramolecular hemiacetals and hemialdals toward more condensed, i.e., also more compact, structures.

Thermograms recorded by differential scanning calorimetry show the endothermic process of dehydration occurring in DAC films during heating (Figure 5b). It is important to note that this process begins way below 100 °C, indicating a chemical dehydration rather than physical vaporization, which would set in at higher temperatures only. This observation is in good agreement with the results of dynamic mechanical analysis (Figure 4a) which show that the films soften already in the first transition, i.e., well below 100 °C. Upon cycling the measurement (Figure 5b) it becomes apparent that the process is not completely reversible. The seconded cycle shows a shift of the endothermic dehydration to higher temperatures due to the loss of water in the first cycle. Similar thermal properties indicating a broad moisture-related event at low temperatures before a high temperature glass transition sets in was previously observed for dialcohol cellulose films.[56]

DH-DAC films largely dehydrated by equilibration over P_4O_{10} (residual water content 1 wt %) did not show this thermal transition in the studied DSC temperature range (<137 °C) which confirms that the endothermic event recorded for DAC films (equilibrated at 65% RH; 6% water content) is indeed the result of dehydration processes.

Heating of DAC film fragments in a closed DSC pan to somewhat higher than 150 °C afforded a conglomerate of the DAC pieces stuck together which suggests melting of the material. On the other hand, some yellow discoloration was observed which was indicative of beginning thermal degradation. Since hot water can act as a solvent for DAC, larger

DOI: 10.1021/acs.biomac.8b00536
Biomacromolecules 2018, 19, 2969−2978

amounts of water can interfere with melting which, in turn, may overlap with the inset of thermal degradation at higher temperatures.

Softening of the material during heating, accommodated by dehydration, enables reshaping of DAC films like it is done in the applied pressing step, which would be particularly useful for industrial fabrication processes.

Light Transmittance. UV/vis spectroscopy confirmed a high light transmittance for all films of this study over the entire range of visible and near-infrared light. Unpressed DAC films (average thickness 128 μm), for example, had a light transmittance of 91% between 400 and 700 nm, which is higher transmittance compared to polycarbonate[54] (PC, Lexan 141, 86−89% at 550 nm) for instance. In the UV range, the transmittance for UVA (320−400 nm) and UVB (290−320 nm) light was 80% and 46%, respectively, and <1% for wavelengths below 267 nm (UVC). Pressing of DAC films (average thickness 86 μm) does virtually not reduce the light transmittance which was still 90% between 400 and 700 nm. Also, reinforcement of the films with 5 wt % CNC (110 μm thickness) caused only a slight reduction of light transmittance for the same wavelength range and was still at 89%.

Oxygen Barrier Properties. All tested 2,3-dialdehyde cellulose films had exceptionally low oxygen transmission rates (OTR), which were clearly below the detection limit of the applied method (0.008 $cm^3\ m^{-2}\ day^{-1}$, 50% RH). The very low oxygen permeability—calculated by multiplying OTR with the thickness of the film and dividing it by the oxygen partial pressure difference (atmospheric pressure)—renders DAC films highly attractive bio-based candidates for packaging applications, where transparent high-performance oxygen barrier materials are desired. Although no exact OP values can be provided for the DAC films owing to the low OTR values obtained even in long-term experiments, it is safe to conclude that the oxygen permeability of all prepared 2,3-dialdehyde films is at least as low as that of commercial poly(ethylene-*co*-vinyl alcohol) films, which are commonly used as oxygen-barrier films and usually have an OP of 0.001 to 0.01 mL μm $m^{-2}\ day^{-1}\ kPa^{-1}$.[57] Furthermore, the prepared DAC films are superior to commercially available films from high-density poly(ethylene), poly(ethylene terephthalate), nylon-6, poly(vinylidene chloride), and poly(vinyl alcohol), which have oxygen permeabilities of 500, 8, 6, 0.4, and 0.04 mL μm $m^{-2}\ day^{-1}\ kPa^{-1}$, respectively, at 0% RH.[58]

The low oxygen permeability of DAC films could be maintained even at a high relative humidity (80% RH; Table 3), which is remarkable because most bio-based films show a strong (exponential) decrease of oxygen barrier properties with increasing relative humidity. For commercial cellophane films, which have an OP value of 0.0481 mL μm $m^{-2}\ day^{-1}\ kPa^{-1}$ at 0% RH, the OP value increases by more than 1 magnitude if the relative humidity rises from 0% RH to 60% RH.[58] Solution-cast films of 2,3-dialdehyde cellulose are also superior to other cellulose-based oxygen barrier materials, such as films from nanofibrillated 6-carboxycellulose—obtained by 2,2,6,6-tetramethyl-1-piperidinyloxyradical-mediated (TEMPO) oxidation of cellulose—which have OP values higher than 0.1 mL μm $m^{-2}\ day^{-1}\ kPa^{-1}$ beyond 35% RH.[59] The OTR and OP values measured and calculated for selected unpressed and pressed DAC films as well as *all*-cellulose DAC/CNC composite films are compiled in Table 3.

Table 4. Oxygen Barrier Properties of DAC Films: Oxygen Transmission Rate (OTR) and Oxygen Permeability (OP) of Selected Unpressed and Pressed Films (Highest Measured Value of OTR and OP) after Equilibration at Different RH

	OTR [$cm^3\ m^{-2}\ day^{-1}$]		OP [mL μm $m^{-2}\ day^{-1}\ kPa^{-1}$]	
	RH 50%	RH 80%	RH 50%	RH 80%
unpressed	<0.008	0.09	<0.006	0.06
pressed	<0.008	0.04	<0.005	0.03
pressed and reinforced (5 wt % CNC)	<0.008	<0.008	<0.009	<0.009

Contact Angle of Water on DAC Films. The initial contact angle (θ_C) of water on DAC film surfaces, measured 15 s after the droplet had been applied, was rather high (about 67°) compared to other cellulosic materials and films. While the calculated θ_C for a crystalline cellulose Iβ surface is 43°,[60] films prepared by spin-coating of cellulose dissolved in *N*-methylmorpholine-*N*-oxide (diluted by DMSO) and thus representing amorphous and semicrystalline cellulose II had water contact angles of 18° to 19° only.[61]

The comparatively high θ_C of the tested DAC films indicates a relatively high hydrophobicity. Following the hypothesis of a reduced amount of hydroxyl groups translating into higher hydrophobicity, the result argues against the existence of larger quantities of aldehyde hydrates (which have two more hydroxyls than an aldehyde) in DAC films and supports—concordant with the results of FTIR, DMA, and DSC analysis and mechanical testing—the assumption that hemiacetals (fewer hydroxyls than the starting moieties: aldehyde hydrate and alcohol) and hemialdals (fewer hydroxyls than the starting moieties: two aldehyde hydrates) play a crucial role for imparting DAC films extraordinarily high stiffness, despite the low molecular weight, flexibility, and polarity of the source biopolymer derivative. The gradual decline of θ_C through absorption of water by DAC films (cf. Figure 4c)—lowering their hydrophobicity—can be seen as confirmation that the intermolecular hemiacetal and hemialdal network formation is reversible, which is highly beneficial with regard to recycling issues.

CONCLUSIONS

Mechanically strong, yet flexible and highly transparent cellulose-based films have been prepared by (1) strong periodate oxidation (DO 92%) of microcrystalline cellulose yielding 2,3-dialdehyde cellulose (DAC), (2) dissolution of DAC in hot water, (3) solution casting, (4) slow oven-drying, and (5) hot pressing. Optionally, the films were reinforced by incorporation of cellulose nanocrystals into the dissolved DAC. The exceptionally good oxygen barrier properties of DAC films even at high humidity, the restriction to water as the only required reaction and processing medium, and the good recyclability of both the cellulose oxidant (sodium periodate) and the DAC films itself render this novel type of bio-based plastics particularly promising and environmental-friendly for packaging applications. Beyond that the moisture-dependent availability of aldehyde moieties and their great reactivity toward amines could be used for further modification of DAC films, such as for immobilization of enzymes,[9] antibodies,[13] or antimicrobial compounds[62] affording substrates for biosensing applications or novel bioactive and functional materials, respectively.

If the aldehyde moieties are not utilized for (surface) modifications, they are predominantly masked as intra- and

DOI: 10.1021/acs.biomac.8b00536
Biomacromolecules 2018, 19, 2969−2978

intermolecular hemiacetal and hemialdal moieties, cross-linking the rather short DAC polymer chains ($M_w \sim 6000$ g mol^{-1}). This unique mechanism greatly contributes to the excellent mechanical properties (Young's modulus 3.4−4.0 GPa, UTS 81−122 MPa) of DAC films. FTIR spectroscopy complemented by dynamic mechanical analysis, differential scanning calorimetry, and tensile testing disclosed important information about the solid-state structure of DAC films and the impact of moisture that governs the hydration state of aldehyde moieties. While dehydration and pressing of DAC films strongly favors the formation of (cyclic) intra- and intermolecular hemiacetal and hemialdal moieties in general, the residual water content of the films limiting aldehyde hydration has a great impact on mechanical properties of the films. In particular elongation at break and toughness can be considerably increased (beyond 600×10^4 J m^{-3}) by dehydration of DAC films. Temperature-induced softening in moist hydrated state is another valuable feature of DAC films allowing for facile material shaping. The relatively high initial contact angle of a water droplet deposited on the surface of the DAC films (~67°) revealed increased hydrophobicity relative to other cellulosic materials and films.

AUTHOR INFORMATION

Corresponding Author

*E-mail falk.liebner@boku.ac.at (F.W.L.).

ORCID

Sven F. Plappert: 0000-0003-3210-3859
Antje Potthast: 0000-0003-1981-2271
Thomas Rosenau: 0000-0002-6636-9260
Falk W. Liebner: 0000-0002-8244-8153

Notes

The authors declare no competing financial interest.

ACKNOWLEDGMENTS

The financial support by the Austrian Science Fund (FWF: I848-N17), the French Agence Nationale de la Recherche (ANR-11-IS08-0002 to J.-M. Nedelec; Austrian-French Project CAP-Bone to N. Pircher, S. Plappert, F. Liebner), and the Academy of Finland (project number 268144, K. S. Mikkonen) is gratefully acknowledged. The authors thank Johannes Theiner (Microanalytical Laboratory, University of Vienna) for elemental analysis, Markus Puschenreiter (Institute of Soil Research, University of Natural Resources and Life Sciences, Vienna) for ICP-MS analysis, Irina Sulaeva (Division of Chemistry of Renewable Resources, University of Natural Resources and Life Sciences, Vienna) for SEC analysis, Maia Tenkanen (Unversity of Helsinki) for fruitful discussions, and the Institute of Wood Technology and Renewable Resources (University of Natural Resources and Life Sciences Vienna) for access to hot pressing equipment as well as contact angle, mechanical and thermal testing instrumentation.

REFERENCES

(1) Goetz, L.; Mathew, A.; Oksman, K.; Gatenholm, P.; Ragauskas, A. J. A novel nanocomposite film prepared from crosslinked cellulosic whiskers. *Carbohydr. Polym.* **2009**, *75* (1), 85−89.

(2) Klemm, D.; Kramer, F.; Moritz, S.; Lindstrom, T.; Ankerfors, M.; Gray, D.; Dorris, A. Nanocelluloses: a new family of nature-based materials. *Angew. Chem., Int. Ed.* **2011**, *50* (24), 5438−66.

(3) French, A. D.; Bertoniere, N. R.; Brown, R. M.; Chanzy, H.; Gray, D. G.; Hattori, K.; Glasser, W. Cellulose. In *Kirk-Othmer Encyclopedia of Chemical Technology*, 5th ed.; Seidel, A., Ed.; John Wiley & Sons, Inc.: Hoboken, NJ, 2004−2007; Vol. *5*, pp 360−394.

(4) Perlin, A. S. Glycol-cleavage oxidation. *Adv. Carbohydr. Chem. Biochem.* **2006**, *60*, 183−250.

(5) Kristiansen, K. A.; Potthast, A.; Christensen, B. E. Periodate oxidation of polysaccharides for modification of chemical and physical properties. *Carbohydr. Res.* **2010**, *345* (10), 1264−71.

(6) Koprivica, S.; Siller, M.; Hosoya, T.; Roggenstein, W.; Rosenau, T.; Potthast, A. Regeneration of Aqueous Periodate Solutions by Ozone Treatment: A Sustainable Approach for Dialdehyde Cellulose Production. *ChemSusChem* **2016**, *9* (8), 825−33.

(7) Kim, U.-J.; Wada, M.; Kuga, S. Solubilization of dialdehyde cellulose by hot water. *Carbohydr. Polym.* **2004**, *56* (1), 7−10.

(8) Münster, L.; Vícha, J.; Klofáč, J.; Masař, M.; Kucharczyk, P.; Kuřitka, I. Stability and aging of solubilized dialdehyde cellulose. *Cellulose* **2017**, *24* (7), 2753−2766.

(9) Wu, R.; He, B. H.; Zhao, G. L.; Qian, L. Y.; Li, X. F. Immobilization of pectinase on oxidized pulp fiber and its application in whitewater treatment. *Carbohydr. Polym.* **2013**, *97* (2), 523−9.

(10) Nikolic, T.; Kostic, M.; Praskalo, J.; Pejic, B.; Petronijevic, Z.; Skundric, P. Sodium periodate oxidized cotton yarn as carrier for immobilization of trypsin. *Carbohydr. Polym.* **2010**, *82* (3), 976−981.

(11) Isobe, N.; Lee, D.-S.; Kwon, Y.-J.; Kimura, S.; Kuga, S.; Wada, M.; Kim, U.-J. Immobilization of protein on cellulose hydrogel. *Cellulose* **2011**, *18* (5), 1251−1256.

(12) Girelli, A. M.; Salvagni, L.; Tarola, A. M. Use of lipase immobilized on celluse support for cleaning aged oil layers. *J. Braz. Chem. Soc.* **2012**, *23* (4), 585−592.

(13) Zhang, X.; Shen, G.; Sun, S.; Shen, Y.; Zhang, C.; Xiao, A. Direct immobilization of antibodies on dialdehyde cellulose film for convenient construction of an electrochemical immunosensor. *Sens. Actuators, B* **2014**, *200*, 304−309.

(14) Kanth, S. V.; Ramaraj, A.; Rao, J. R.; Nair, B. U. Stabilization of type I collagen using dialdehyde cellulose. *Process Biochem.* **2009**, *44* (8), 869−874.

(15) Cheng, Y.; Lu, J.; Liu, S.; Zhao, P.; Lu, G.; Chen, J. The preparation, characterization and evaluation of regenerated cellulose/collagen composite hydrogel films. *Carbohydr. Polym.* **2014**, *107*, 57−64.

(16) Lu, T.; Li, Q.; Chen, W.; Yu, H. Composite aerogels based on dialdehyde nanocellulose and collagen for potential applications as wound dressing and tissue engineering scaffold. *Compos. Sci. Technol.* **2014**, *94*, 132−138.

(17) Mu, C.; Guo, J.; Li, X.; Lin, W.; Li, D. Preparation and properties of dialdehyde carboxymethyl cellulose crosslinked gelatin edible films. *Food Hydrocolloids* **2012**, *27* (1), 22−29.

(18) Guo, J.; Li, X.; Mu, C.; Zhang, H.; Qin, P.; Li, D. Freezing-thawing effects on the properties of dialdehyde carboxymethyl cellulose crosslinked gelatin-MMT composite film. *Food Hydrocolloids* **2013**, *33*, 273.

(19) Shen, G.; Zhang, X.; Zhang, S. A Label-Free Electrochemical Aptamer Sensor Based on Dialdehyde Cellulose/Carbon Nanotube/Ionic Liquid Nanocomposite. *J. Electrochem. Soc.* **2014**, *161* (12), B256−B260.

(20) Kimura, S.; Isobe, N.; Wada, M.; Kuga, S.; Ko, J.-H.; Kim, U.-J. Enzymatic hydrolysis of chitosan-dialdehyde cellulose hydrogels. *Carbohydr. Polym.* **2011**, *83* (4), 1850−1853.

(21) Liu, X. D.; Nishi, N.; Tokura, S.; Sakairi, N. Chitosan coated cotton fiber: preparation and physical properties. *Carbohydr. Polym.* **2001**, *44* (3), 233−238.

(22) Kim, U.-J.; Kuga, S. Ion-exchange separation of proteins by polyallylamine-grafted cellulose gel. *J. Chromatogr. A* **2002**, *955* (2), 191−196.

(23) Doughan, S.; Uddayasankar, U.; Krull, U. J. A paper-based resonance energy transfer nucleic acid hybridization assay using upconversion nanoparticles as donors and quantum dots as acceptors. *Anal. Chim. Acta* **2015**, *878*, 1−8.

(24) Kim, U.-J.; Kuga, S. Thermal decomposition of dialdehyde cellulose and its nitrogen-containing derivatives. *Thermochim. Acta* **2001**, *369* (1−2), 79−85.

DOI: 10.1021/acs.biomac.8b00536
Biomacromolecules 2018, 19, 2969−2978

(25) Maekawa, E.; Koshijima, T. Preparation and Structural Consideration of Nitrogen-Containing Derivatives Obtained from Dialdehyde Cellulose. *J. Appl. Polym. Sci.* **1991**, *42*, 169.
(26) Sabzalian, Z.; Alam, M. N.; van de Ven, T. G. M. Hydrophobization and characterization of internally crosslink-reinforced cellulose fiber. *Cellulose* **2014**, *21*, 1381−1393.
(27) Visanko, M.; Liimatainen, H.; Sirvio, J. A.; Heiskanen, J. P.; Niinimaki, J.; Hormi, O. Amphiphilic cellulose nanocrystals from acid-free oxidative treatment: physicochemical characteristics and use as an oil-water stabilizer. *Biomacromolecules* **2014**, *15* (7), 2769−75.
(28) Visanko, M.; Liimatainen, H.; Sirviö, J. A.; Mikkonen, K. S.; Tenkanen, M.; Sliz, R.; Hormi, O.; Niinimäki, J. Butylamino-functionalized cellulose nanocrystal films: barrier properties and mechanical strength. *RSC Adv.* **2015**, *5* (20), 15140−15146.
(29) Espigares, I.; Elvira, C.; Mano, J. F.; Vázquez, B.; San Román, J.; Reis, R. L. New partially degradable and bioactive acrylic bone cements based on starch blends and ceramic fillers. *Biomaterials* **2002**, *23* (8), 1883−1895.
(30) Verma, V.; Verma, P.; Ray, P.; Ray, A. R. 2,3-Dihydrazone cellulose: Prospective material for tissue engineering scaffolds. *Mater. Sci. Eng., C* **2008**, *28* (8), 1441−1447.
(31) Li, J.; Wan, Y.; Li, L.; Liang, H.; Wang, J. Preparation and characterization of 2,3-dialdehyde bacterial cellulose for potential biodegradable tissue engineering scaffolds. *Mater. Sci. Eng., C* **2009**, *29* (5), 1635−1642.
(32) Syamala Devi, K.; Sinha, T. J.; Vasudevan, P. Biosoluble surgical material from 2,3-dialdehyde cellulose. *Biomaterials* **1986**, *7* (3), 193−6.
(33) Potthast, A.; Schiehser, S.; Rosenau, T.; Kostic, M. Oxidative modifications of cellulose in the periodate system − Reduction and beta-elimination reactions 2nd ICC 2007. *Holzforschung* **2009**, DOI: 10.1515/HF.2009.108.
(34) Morooka, T.; Norimoto, M.; Yamada, T. Periodate oxidation of cellulose by homogeneous reaction. *J. Appl. Polym. Sci.* **1989**, *38* (5), 849−858.
(35) Process Development Center Cellulose Nanocrystals; http://umaine.edu/pdc/cellulose-nano-crystals/ (13.06.2017).
(36) Maekawa, E.; Koshijima, T. Properties of 2,3-dicarboxy cellulose combined with various metallic ions. *J. Appl. Polym. Sci.* **1984**, *29* (7), 2289−2297.
(37) Sulaeva, I.; Klinger, K. M.; Amer, H.; Henniges, U.; Rosenau, T.; Potthast, A. Determination of molar mass distributions of highly oxidized dialdehyde cellulose by size exclusion chromatography and asymmetric flow field-flow fractionation. *Cellulose* **2015**, *22* (6), 3569−3581.
(38) Varma, A. J.; Kulkarni, M. P. Oxidation of cellulose under controlled conditions. *Polym. Degrad. Stab.* **2002**, *77* (1), 25−27.
(39) Moulay, S. Molecular iodine/polymer complexes. *J. Polym. Eng.* **2013**, DOI: 10.1515/polyeng-2012-0122.
(40) Siller, M.; Amer, H.; Bacher, M.; Roggenstein, W.; Rosenau, T.; Potthast, A. Effects of periodate oxidation on cellulose polymorphs. *Cellulose* **2015**, *22* (4), 2245.
(41) Fan, Q. G.; Lewis, D. M.; Tapley, K. N. Characterization of cellulose aldehyde using Fourier transform infrared spectroscopy. *J. Appl. Polym. Sci.* **2001**, *82* (5), 1195−1202.
(42) Sirvio, J. A.; Liimatainen, H.; Visanko, M.; Niinimaki, J. Optimization of dicarboxylic acid cellulose synthesis: reaction stoichiometry and role of hypochlorite scavengers. *Carbohydr. Polym.* **2014**, *114*, 73−7.
(43) Ishak, M. F.; Painter, T.; Andersen, V. S.; Enzell, C. R.; Lousberg, R. J. J. C.; Weiss, U. Formation of Inter-residue Hemiacetals During the Oxidation of Polysaccharides by Periodate Ion. *Acta Chem. Scand.* **1971**, *25*, 3875−3877.
(44) Mester, L. The Formazan Reaction in Proving the Structure of Periodate Oxidized Polysaccharides. *J. Am. Chem. Soc.* **1955**, *77* (20), 5452−5453.
(45) Painter, T.; Larsen, B.; Silvennoinen, K.; Vaahtera, K.; Shimizu, A. Kinetic Evidence for Inter-residue Hemiacetal Formation during the Oxidation of Amylose by Periodate Ion. *Acta Chem. Scand.* **1970**, *24*, 2724−2736.
(46) Smidsrød, O.; Larsen, B.; Painter, T.; Solymosy, F.; Shimizu, A. Monte-Carlo Investigation of Nearest-neighbour Auto-inhibitory Effects in the Oxidation of Amylose by Periodate Ion. *Acta Chem. Scand.* **1970**, *24*, 3201−3212.
(47) Painter, T. J. Preparation and periodate oxidation of C-6-oxycellulose: conformational interpretation of hemiacetal stability. *Carbohydr. Res.* **1977**, *55* (1), 95−103.
(48) Guigo, N.; Mazeau, K.; Putaux, J.-L.; Heux, L. Surface modification of cellulose microfibrils by periodate oxidation and subsequent reductive amination with benzylamine: a topochemical study. *Cellulose* **2014**, *21* (6), 4119−4133.
(49) Azizi Samir, M. A.; Alloin, F.; Dufresne, A. Review of recent research into cellulosic whiskers, their properties and their application in nanocomposite field. *Biomacromolecules* **2005**, *6* (2), 612−26.
(50) Jalal Uddin, A.; Araki, J.; Gotoh, Y. Toward "strong" green nanocomposites: polyvinyl alcohol reinforced with extremely oriented cellulose whiskers. *Biomacromolecules* **2011**, *12* (3), 617−24.
(51) Wang, B.; Torres-Rendon, J. G.; Yu, J.; Zhang, Y.; Walther, A. Aligned bioinspired cellulose nanocrystal-based nanocomposites with synergetic mechanical properties and improved hygromechanical performance. *ACS Appl. Mater. Interfaces* **2015**, *7* (8), 4595−607.
(52) Kim, U.-J.; Kuga, S.; Wada, M.; Okano, T.; Kondo, T. Periodate Oxidation of Crystalline Cellulose. *Biomacromolecules* **2000**, *1* (3), 488−492.
(53) Mark, J. E. *Polymer Data Handbook*; Oxford University Press: New York, 1999.
(54) Polycarbonates. In *Kirk-Othmer Encyclopedia of Chemical Technology*, 5th ed.; Kirk-Othmer, R. E., Ed.; Wiley-Interscience: 2006; Vol. *19*.
(55) Engelberg, I.; Kohn, J. Physico-mechanical properties of degradable polymers used in medical applications: A comparative study. *Biomaterials* **1991**, *12* (3), 292−304.
(56) Kasai, W.; Morooka, T.; Ek, M. Mechanical properties of films made from dialcohol cellulose prepared by homogeneous periodate oxidation. *Cellulose* **2014**, *21* (1), 769−776.
(57) Wu, C. N.; Saito, T.; Fujisawa, S.; Fukuzumi, H.; Isogai, A. Ultrastrong and high gas-barrier nanocellulose/clay-layered composites. *Biomacromolecules* **2012**, *13* (6), 1927−32.
(58) Yang, Q.; Fukuzumi, H.; Saito, T.; Isogai, A.; Zhang, L. Transparent cellulose films with high gas barrier properties fabricated from aqueous alkali/urea solutions. *Biomacromolecules* **2011**, *12* (7), 2766−71.
(59) Shimizu, M.; Saito, T.; Fukuzumi, H.; Isogai, A. Hydrophobic, ductile, and transparent nanocellulose films with quaternary alkylammonium carboxylates on nanofibril surfaces. *Biomacromolecules* **2014**, *15* (11), 4320−5.
(60) Mazeau, K.; Rivet, A. Wetting the (110) and (100) surfaces of Ibeta cellulose studied by molecular dynamics. *Biomacromolecules* **2008**, *9* (4), 1352−4.
(61) Eriksson, M.; Notley, S. M.; Wagberg, L. Cellulose thin films: degree of cellulose ordering and its influence on adhesion. *Biomacromolecules* **2007**, *8* (3), 912−9.
(62) Hou, Q.; Liu, W.; Liu, Z.; Duan, B.; Bai, L. Characteristics of antimicrobial fibers prepared with wood periodate oxycellulose. *Carbohydr. Polym.* **2008**, *74* (2), 235−240.

DOI: 10.1021/acs.biomac.8b00536
Biomacromolecules 2018, 19, 2969−2978